Supported Metal Nanoparticle Catalysts and Electrocatalysts: Correlating Structure with Function through Energetics

Nanoparticles of late transition metals are used as catalysts and electrocatalysts for industrial chemical reactions that produce fuels, convert them to electricity and clean up pollution associated with the generation and use of fuels. For such applications, they usually are bonded onto the surfaces of oxide or carbon support materials. To provide the energy needed for sustained economic development, we must develop new and improved solid catalysts and electrocatalysts for a variety of reactions that take better advantage of traditional and alternate energy sources (solar, wind, biomass or nuclear) and avoid serious environmental problems.

We propose here an experimental research program aimed to provide the basic understanding needed to develop new and improved catalysts and electrocatalysts for a variety of reactions that involve nanoparticles of late transition metals supported on oxide and carbon materials. Specifically, we will study well-defined model catalysts consisting of metal and bimetallic nanoparticles supported on single-crystalline oxide, mixed-oxide and carbon surfaces, structurally characterized using a variety of ultrahigh vacuum surface science techniques. We will use calorimetry techniques invented here and available nowhere else in the world to measure the energies of the metal atoms in these particles, the metal/support adhesion energies and the energy of adsorbed intermediates on these particles.

Our prior results showed that the chemical potential of the metal atoms in the particles, which we measure directly by metal adsorption calorimetry, is an important descriptor for catalytic performance. For particles smaller than 6 nm, it depends strongly on their size and the nature of the oxide or carbon support upon which the particles sit, and correlates with their catalytic performance (resistance to sintering, bond energies to adsorbed catalytic reaction intermediates, catalytic activity and selectivity). Our prior results led us to a quantitative relationship that accurately predicts metal chemical potential versus particle size and the metal / support adhesion energy (E_{adh}). Thus, knowing how E_{adh} varies with the metal and support material is crucial to predicting metal chemical potential for different catalyst materials, and thus their catalytic performance. We also discovered how to predict E_{adh} for different metals on a given oxide support, once E_{adh} is known for one metal.

We propose to refine these relationships, extending them to other oxides and carbon supports, thus enabling predictions of adhesion energies for new metal/support combinations without measurement. We will also measure quantitative relationships between metal chemical potential and catalytic properties for metals in model structures where their chemical potential is tuned by independently varying the particle size and the support strength, and by alloying with other metals. We will correlate this tuned chemical potential with (1) calorimetrically-measured adsorption energies of two important and ubiquitous adsorbed catalytic intermediates ($-CH_3$, $-OCH_3$) on these nanoparticles, and (2) their sintering rates. We will also measure the adsorption energies of metal monomers on these supports, which are crucial parameters in kinetic models for sintering rates.

The proposed work will provide the basic understanding needed to develop better catalyst materials for clean, sustainable energy technologies. These measured energies will also provide key benchmarks (that cannot be provided by any other laboratory, nor by any theoretical methods currently available) needed for developing more accurate computational tools for heterogeneous catalysis and surface science. A marked improvement is such computational tools would revolutionize research in many areas.

I. Introduction

Nanoparticles of late transition metals dispersed across support materials form the basis for a wide variety of catalysts, electrocatalysts and photocatalysts that are either currently used industrially for energy, chemical and environmental technologies, or hold promise for such applications in the future. It is well known that the rates (per surface metal atom) and selectivities of catalytic, electrocatalytic and photocatalytic reactions often depend strongly upon both the particle size and the nature of the material upon which they are supported, especially when the particles are smaller than ~6 nm in diameter.[1-17] A holy grail of catalysis research is to understand, at a predictive level, how particle size and support affect activity and selectivity for a given catalytic metal. A common problem with such catalysts is that they deactivate with time-on-stream by sintering (also called coarsening), whereby the particles increase in average size and diminish in number. Another major goal of catalysis research is to be able to predict how catalyst structure can be altered to enhance sintering resistance.[P12]

We have recently proven that both catalytic reactivity and the rate of catalyst sintering correlate strongly with the chemical potential of the metal atoms in these supported metal particles.[18-22][P2,P6,P12] The definition of "chemical potential" underlies the reason for using these particular words to describe this highly important thermodynamic property: It describes the potential of a given species (in this case, metal atoms) to do chemistry. The higher its chemical potential, the less stable and thus the more reactive it is. In terms of "higher reactivity" for metal atoms, we refer here both to their strength of adsorption of small molecules and their rate of deactivation by sintering. Thus, metal chemical potential is one very important descriptor for understanding and even predicting catalytic performance.

Let us consider first sintering rates, where the relationship to metal chemical potential is already quantitatively established. The loss of activity over long time due to sintering is a huge problem in catalysis,[22-29] so there has been much work in developing models that predict the rate of sintering. The goal is to be able to predict particle sizes at the long times needed for industrial applications (~1 year) based on short-term measurements of size versus time.[21, 30] In general, the sintering rates of individual particles has been shown to increase with $\mu(R)$, the chemical potential of metal atoms in that particle, which itself is a function of the particle radius R (or "effective radius" for particles that are not partial spheres, defined such that the particle's volume equals that for a hemisphere of that radius). Here we define the reference state of zero chemical potential such that $\mu(R)$ is the chemical potential relative to that for an infinitely large particle of the same metal (i.e., for bulk metal(solid)). As an example of a sintering rate equation, we developed a model for sintering rates [21, 22] that is based on an atomistic mechanism originally developed by Wynblatt and Gjostein [31]. When Ostwald ripening is the dominant mechanism, the radius of any given particle at any time changes with a rate [21, 22]:

$$\frac{dR}{dt} = \frac{K}{R}\left(\exp\left[\frac{-E_{tot}}{kT}\right]\right)\left(\exp\left[\frac{\mu(R^*)}{kT}\right] - \exp\left[\frac{\mu(R)}{kT}\right]\right) \quad (1)$$

where K and E_{tot} are system-dependent constants, and R* is the equilibrium radius for the concentration of diffusing monomers at that time. This concentration is determined by the entire size distribution of particles. Particles with $R < R^*$ (radius smaller than this critical radius) get smaller with time, and those with $R > R^*$ get larger. *The rates at which this happens for a given radius is a very strong function of $\mu(R)$ in a way very similar to it making a negative contribution to the activation energy* [21, 22]. The higher $\mu(R)$ is for a small particle, the faster it gets smaller. Our more recent measurements of chemical potentials of metals on more strongly interacting supports

like CeO_2 (where $\mu(R)$ is lower for a given R) and their comparisons to sintering rates have further verified the validity of this rate expression.[19, 32]

This rate expression was derived assuming that monomer detachment from the particle is rate determining. The values E_{tot} and K are combinations of prefactors and energies for elementary atom-migration steps. They depend on fundamental properties of the metal and the support, such as the energy difference between a metal atom when it is an isolated monomer on the support surface versus when present in a metal particle of infinite size. The sintering kinetic model in [21, 22] was further improved by Datye's group[33] by improving the way $\mu(R^*)$ is calculated.

The factor $e^{\mu(R)/kT}$ in Eq. (1) also appears in a variety of other rate expressions for sintering kinetics derived assuming different elementary steps control the rate instead. [21] Other kinetic models for sintering mechanisms are required when the rate is dominated by particle diffusion / agglomeration instead of Ostwald ripening, and that mechanism sometimes dominates under certain conditions.[P12] This factor $e^{\mu(R)/kT}$ also appears directly in the rate expression for sintering by that alternate mechanism, at least in some derivations based on an atomistic mechanism.[21]

A consequence of metal chemical potential that is even more important than its effect on sintering rates is its effect on the reactivity of supported nanoparticles in their interactions with gases, e.g., when binding adsorbed catalytic reaction intermediates. We have pointed out, with numerous examples, that the same metal atoms will bind small adsorbates more strongly when they are in a structure with high chemical potential, and more weakly when in a structure with lower chemical potential.[18, 19, 34] Thus, when present in the form of tiny (1-2 nm effective diameter) nanoparticles, where the metal chemical potential is very high,[18, 19, 34] they bind small adsorbates more strongly than large particles or bulk metal.[18, 19, 34, 35] For example, oxygen adatoms bind to ~1 nm Au nanoparticles on TiO_2(110) so strongly that the activation energy for their desorption as O_2 is ~50 kJ/mol O_2 (~40%) higher than from bulk Au single crystal surfaces [20]. The dominant effect here is associated with the fact that the surface metal atoms are more coordinatively-unsaturated on smaller particles, as investigated in detail by DFT on unsupported Au and Pt clusters from 13 to 1415 atoms, or ~0.7−3.6 nm in diameter,[36, 37] which is the same reason step edges usually bind small adsorbates more strongly than close-packed terraces. Conversely, when metal atoms are present in certain bimetallic surfaces where they are more stable (i.e., have lower chemical potential) than in the pure bulk metal (e.g., when combined with other metals with which they make highly exothermic alloys), they bind adsorbates more weakly than the surface of the pure bulk metal.[18, 19, 38, 39] For example, for a Pd monolayer on Ta(110), the isosteric heat of adsorption of CO is smaller than on pure Pd(111) by ~63 kJ/mol (~40%), and the TPD peak for adsorbed CO is shifted by more than 200 K to lower temperature [38]. Rodriguez and Goodman[40] showed that for seven such metal-on-metal systems involving Pd and Ni monolayers, the more stable the Ni or Pd monolayer (as estimated by its peak temperature in temperature programmed desorption (TPD) from the underlying metals), the more weakly it adsorbs CO (as estimated by the CO TPD peak temperature). Recent DFT calculations by Abild-Petersen's group have shown a similar trend for later transition metal atoms in metal surfaces: the higher the energy cost to remove that metal atom from the solid, the more weakly it bonds –OH and $–CH_3$ groups.[41] It is clear that the thermodynamic stability of metal atoms correlates in many systems with their chemical reactivity: The higher the metal's chemical potential, the more strongly it bonds small adsorbates. (This is true in chemisorption, but likely to break down when van der Waals interactions dominate the adsorption energy rather than usual chemisorption bonds, since larger metal particles should have higher polarizability.)

It is clear that metal chemical potential is a powerful descriptor for catalytic performance, whether with regards to the catalyst's chemical reactivity or its long-term resistance to deactivation by sintering. Thus, there is strong motivation to develop predictive ability in estimating metal chemical potential in catalyst nanostructures. This goes hand-in-hand with the goal of developing a fundamental understanding of such oxide- and carbon-supported metal catalysts, in particular the relationships amongst the atomic-level structural properties of these complex nanomaterials and their catalytic performance properties, namely activity, selectivity and long-term stability under reaction conditions. We propose an experimental research program that will provide a basic understanding of these relationships, particularly by developing quantitative relationships between the key structural properties of the catalyst material (i.e., metal nanoparticle size, chemical composition of the support material, particle-particle separation) and the calorimetrically-measured stability (or chemical potential) of the metal atoms in the particles. We will then develop more quantitative correlations between this chemical potential and the catalytic performance properties of these materials.

We will study model catalysts which are structurally very well defined, consisting of size-controlled metal and bimetallic nanoparticles on clean surfaces of single-crystalline oxide and carbon supports. We bring to this our unique abilities for calorimetric measurements on such model catalysts, which provide both the energies of the surface metal atoms that make up the catalyst material itself and the strength with which they bond adsorbed intermediates.

Our proposed experiments are designed to first clarify the structural factors that control the chemical potential of catalytic metal atoms in supported nanoparticles. Our recent calorimetry measurements under this DOE grant have proven that for monometallic particles, this chemical potential increases very strongly with decreasing particle diameter (D) below ~6 nm. An example for Ag on slightly reduced CeO_2(111) is shown in Fig. 1. The magnitude of the change is huge (~80 kJ/mol), and thus it has dramatic consequences for catalytic performance, as described above. We first derived a Gibbs-Thomson-like relation proving that the chemical potential of metal atoms in a large hemispherical particle of diameter D on support material A differs from that in the bulk of the metal by:[P2]

$$\mu(D) = (3\gamma_m - E_{adh})(2V_m / D), \quad (1)$$

where γ_m is the surface energy of the bulk metal, E_{adh} is the adhesion energy at the bulk metal / oxide interface, and V_m is the molar volume of the bulk metal. By comparing to our calorimetric measurements of metal atom chemical potential on oxide-supported metal nanoparticles as a function of particle size for five different metal / oxide combinations, we found that our measured chemical potential exceeds that predicted bt Eq. (1) when the particles get smaller than ~5 nm, and especially below 2 nm (see Fig. 1). For late transition metals on all the oxides studied, we showed a very good fit to the measured values for particles down to only a few atoms by a modified version of Eq. (1):[P6]

$$\mu(D) = [(3\gamma_m - E_{adh})(1 + D_o/D)](2V_m / D), \quad (2)$$

where D_o is a constant for all systems equal to ~1.5 nm. The added factor $(1 + D_o/D)$ is an empirical correction that accounts for the fact that both the metal's surface energy and E_{adh} increase rather strongly with decreasing size when D drops below 5 nm. The surface energy increases due to the increasing fraction of coordinatively-unsaturated surface metal atoms (e.g., step, kink and corner sites).[22][P6] An example of the high quality of fit is shown in Fig. 1.

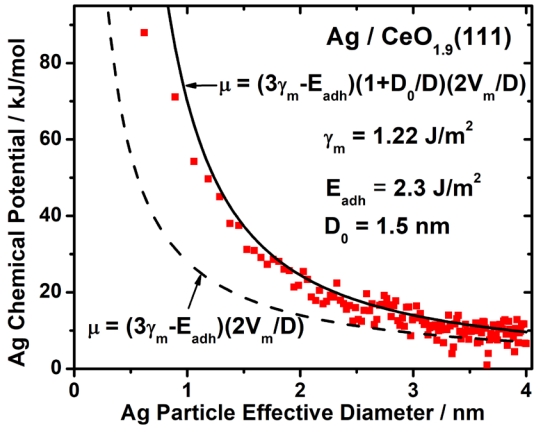

Figure 1. The chemical potential of Ag atoms in Ag nanoparticles on slightly reduced CeO_2(111) measured by calorimetry compared to Eq. (2), using an independently-determined value for E_{adh}. Here, D_0 is a fit parameter that was chosen not for this curve alone, but to simultaneously fit five different metal / oxide combinations.[P6] Also shown is the prediction of Eq. (1), which we derived assuming that γ_m and E_{adh} stay constant at their known values for the large-size limit and which clearly fails below 4 nm.[P2]

Since γ_m and V_m are well known for all late transition metals, all one needs to know to gain predictive ability for the chemical potential versus particle size for a given support is E_{adh}. Thus, there is great motivation to learn what factors control metal/support adhesion energies. Knowing these becomes even more important when one recognizes that E_{adh} also determines the equilibrium shape of the metal particle,[18] and shape also effects catalytic activity and selectivity.[42-44] We therefore propose to continue our systematic study of the factors that control E_{adh} and the metal's chemical potential versus particle size, using the same calorimetric method as we have used in Fig. 1.

As shown in Fig. 2, on the basis of such calorimetric measurements, we have proven that, *for a given oxide surface, E_{adh} increases linearly from metal to metal with increasing magnitude of the heat of formation of the most stable oxide of the metal from metal gas plus O_2*, per mole of metal (i.e., $\Delta H_{sub,M}$-$\Delta H_{f,MOx}$, where $\Delta H_{sub,M}$ is the metal's heat of sublimation and $\Delta H_{f,MOx}$ is the standard heat of formation of the most stable bulk oxide of that metal, per mole of metal). This factor is what we proposed as a convenient descriptor of the oxophilicity of the gaseous metal atom, since it directly reflects the strength of the chemical bonds this metal atom can make to oxygen. It is divided by $V_M^{2/3}$ (where and V_M is the volume per mole in the bulk metal solid) to convert this energy from "per mole" to "per unit area", i.e., the units of E_{adh}. Importantly, we had published this correlation earlier,[P2] but have added here our new (unpublished) points for Ni. This is the most oxophilic metal studied, so these Ni points are the ones farthest to the right. That these new Ni points fit so closely to the lines extrapolated from our earlier correlation *provides a strong proof that this linear scaling relation actually has predictive ability even well outside the range where we first developed it*. Indeed, proving this was one of our motivations for studying Ni on these two oxides, as stated in our proposal three years ago.

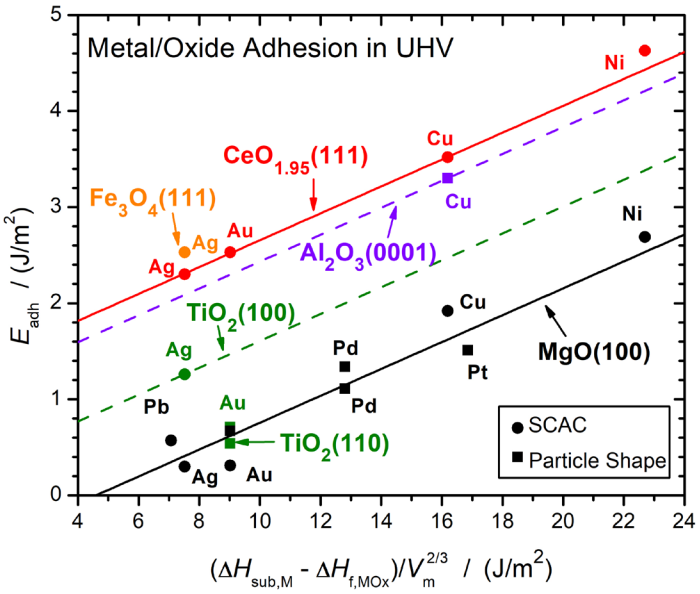

Figure 2. Experimental adhesion energies of different metals (as continuous films or for the largest nanoparticles studied) to various oxide surfaces plotted versus $[(\Delta H_{sub,M}-\Delta H_{f,MOx})/N_A] / V_M^{2/3}$, which is a measure of the oxophilicity of the metal atom per unit surface area (see text). These measurements were all done in ultrahigh vacuum (UHV) on clean oxide surfaces, using either our calorimetry (SCAC) or particle-shape measurements by electron microscopy or grazing-incidence Xray scattering.

This is by far the most extensive collection of adhesion energies ever reported for clean metal/oxide interfaces. This correlation proves that metal-oxygen bonds dominate interfacial bonding. This is consistent with density-functional theory (DFT) calculations of isolated metal adatoms, which show they bind most strongly to oxygen anion sites of these oxide surfaces (when no vacancies are present)[18, 45, 46]. For the two different stoichiometric oxide surfaces studied with multiple different metals in Fig. 2 (MgO(100) and CeO_2(111)), the slopes of their correlations (i.e., metal adhesion energy vs oxophilicity) are nearly the same, but their offsets are very different (CeO_2(111) > MgO(100) by 2 J/m^2). This suggests that the slope is nearly independent of oxide. We propose below to further confirm this constant slope with measurements on other oxides. If verified, it will allow estimations of adhesion energies for many metals on a given oxide based on measurement of only one metal, as suggested by the dashed line in Fig. 2 for α-Al_2O_3(0001) based on a single measurement on Cu.

Even before these new points in Fig. 2, the power of this linear scaling we discovered was recognized by the community and extended. For example, O'Connor et al.[47] showed that the DFT-calculated adsorption energies of 12 different transition metals as isolated adatoms on MgO(100), CeO_2(111), CeO_2(110), TiO_2(011), ZnO(100), TbO_2(111) and α -Al_2O_3(0001) also scale linearly with $(\Delta H_{sub,M}-\Delta H_{f,MOx})$, and cited our prior DOE work for introducing this as the appropriate descriptor.

The offsets of the lines in Fig. 2 show that, *for a given metal, its adhesion energies to different oxides (i.e., the offset between lines in Fig. 2) are quite different.* We have been unable to fully explain these differences, in spite of finding a rough correlation.[P6-7] Our new data point for Ag on rutile-TiO_2(100) in Fig. 2 (also not yet published) is well above the point for Au on rutile-TiO_2(110), suggesting that the adhesion energy line for the (100) face of rutile is higher than that for its (110) face. This can be qualitatively explained by the proposal we made previously [P6-7] that E_{adh} increases in proportion to the number of coordinatively-unsaturated surface O anions per unit area (which is 40% higher on the (100) face), and thus adds support to that proposal. That proposal was based on our demonstration that the interfacial bonding is mainly between metal atoms of the metal nanoparticle and surface O atoms of the oxide (to explain the lines in Fig. 2, as noted above).

We propose experiments designed to further clarify how these adhesion energy trend lines in Fig. 2 vary between different oxide surfaces for the same metal.

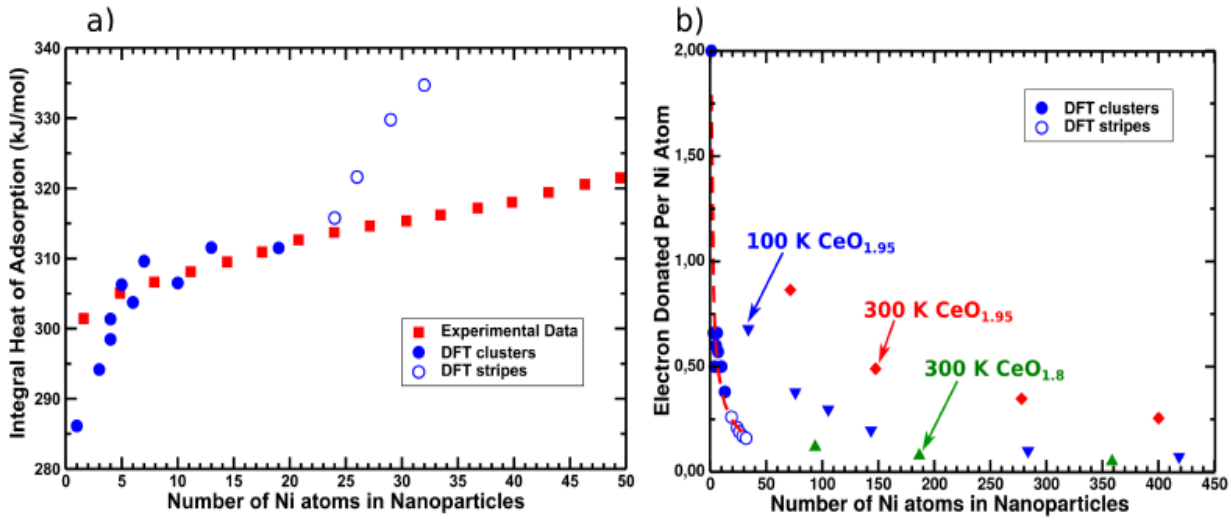

Figure 3. (a) Integral heats of Ni adsorption (per mole of Ni atoms) on CeO_2(111) terraces at 100 K, and (b) cumulative number of electrons donated to ceria per Ni atom, both as function of the number of Ni atoms in the Ni_n clusters. The DFT heats are shifted down by 88 kJ/mol to correct for systematic errors in DFT energies. For n > 20, the Ni_n aggregates in DFT correspond to continuous 1D Ni islands ("stripes"), so they are really infinitely larger than indicated on the x axis, which lists the Ni atoms per unit cell for these stripes (open circles). The experimental differential heats further increase to 390 kJ/mol by 3 nm diameter and to the heat of bulk Ni sublimation (430 kJ/mol) for the largest particles (not shown).

II.H. Publications which Acknowledge Support from this Grant *(since submission of the previous proposal in Nov. 2016).*

A. Publications Resulting from this DOE Grant Support alone.

P1. Calorimetric Measurement of Adsorption and Adhesion Energies of Cu on Pt(111), T. E. James, S. L. Hemmingson, J. R.V. Sellers and C. T. Campbell, ***Surface Science*** 657, 58–62 (2017) (Selected as *Editor's Choice*). DOI: 10.1016/j.susc.2016.10.012.

P2. Trends in Adhesion Energies of Metal Nanoparticles on Oxide Surfaces: Understanding Support Effects in Catalysis and Nanotechnology, S. L. Hemmingson and C. T. Campbell, ***ACS Nano*** 11, 1196-1203 (2017). DOI: 10.1021/acsnano.6b07502. (36 citations)

P3. Correction to: "Trends in Adhesion Energies of Metal Nanoparticles on Oxide Surfaces: Understanding Support Effects in Catalysis and Nanotechnology", S. L. Hemmingson and C. T. Campbell, ***ACS Nano*** 11, 1196-1203 (2017), *ACS Nano* 11, 4373 (2017).

P4. Energetics of 2D and 3D Gold Nanoparticles on MgO(100): Influence of Particle Size and Defects on Gold Adsorption and Adhesion Energies, S. L. Hemmingson, G. M. Feeley, N. J. Miyake and C. T. Campbell, ***ACS Catalysis*** 7, 2151-2163 (2017) DOI: 10.1021/acscatal.6b03173.

P5. The Degree of Rate Control: A Powerful Tool for Catalysis Research, C. T. Campbell, ***ACS Catalysis*** *(Invited Viewpoint)* 7, 2770-2779 (2017). DOI: 10.1021/acscatal.7b00115. (63

citations)

P6. The Chemical Potential of Metal Atoms in Supported Nanoparticles: Dependence upon Particle Size and Support, Charles T. Campbell and Zhongtian Mao, ***ACS Catalysis*** 7, 8460-8466 (2017). DOI:10.1021/acscatal.7b03090. (22 citations)

P7. Correction to "The Chemical Potential of Metal Atoms in Supported Nanoparticles: Dependence upon Particle Size and Support", Charles T. Campbell and Zhongtian Mao, *ACS Catalysis* 2017, 7, 8460-8466. Charles T. Campbell and Zhongtian Mao, ***ACS Catalysis*** 8, 8763−8764 (2018).

P8. Energetics of Au adsorption and film growth on Pt(111) by single-crystal adsorption calorimetry, Gabriel M. Feeley, Stephanie L. Hemmingson and Charles T. Campbell, ***Journal of Physical Chemistry C*** 123, 5557-5561 (2019). DOI: 10.1021/acs.jpcc.9b00018.

P9. Apparent Activation Energies in Complex Reaction Mechanisms: A Simple Relationship via Degrees of Rate Control, Zhongtian Mao and Charles T. Campbell, ***ACS Catalysis*** 9, 9465−9473 (2019). DOI: 10.1021/acscatal.9b02761.

P10. The Degree of Rate Control of Catalyst-Bound Intermediates in Catalytic Reaction Mechanisms: Relationship to Site Coverage, Zhongtian Mao and Charles T. Campbell, ***Journal of Catalysis*** 381, 53–62 (2020). DOI: 10.1016/j.jcat.2019.09.044.

P11. Kinetic Isotope Effects: Interpretation and Prediction Using Degrees of Rate Control, Zhongtian Mao and Charles T. Campbell, *ACS Catalysis* **10**, 4181−4192 (2020). (Also selected for inclusion in the *ACS Catalysis* Virtual Issue: Blurring the Lines Between Catalysis Subdisciplines.) https://dx.doi.org/10.1021/acscatal.9b05637

P12. Energetics and Structure of Ni Atoms and Nanoparticles on MgO(100), Zhongtian Mao, Wei Zhao, Ziareena Al-Mualem and Charles T. Campbell, *Journal of Physical Chemistry C* **124**, 14685−14695 (2020). https://dx.doi.org/10.1021/acs.jpcc.0c03468

P13. Calorimetric Metal Vapor Adsorption Energies for Characterizing Industrial Catalyst Support Materials, Wei Zhang and Charles T. Campbell, *J. Catalysis* **392**, 209–216 (2020). https://doi.org/10.1016/j.jcat.2020.09.022

P14. Energetics of Ag Adsorption on and Adhesion to Rutile TiO_2(100) Studied by Microcalorimetry, Zhongtian Mao, John R. Rumptz, and Charles T. Campbell, *Journal of Physical Chemistry C* (submitted)

B. Publications jointly funded by this DOE grant <u>and</u> other grants of the PI and/or his co-authors.

P15. Electrocatalytic Hydrogenation of Phenol over Platinum and Rhodium: Unexpected Temperature Effects Resolved, N. Singh, Y. Song, O. Y. Gutiérrez, D. M. Camaioni, C. T. Campbell, J. A. Lercher, ***ACS Catalysis*** 6, 7466–7470 (2016). DOI: 10.1021/acscatal.6b02296. (34 citations)

P16. The physical chemistry and materials science behind sinter-resistant catalysts, Yunqian Dai, Ping Lu, Charles T. Campbell and Younan Xia, ***Chemical Society Reviews*** 47, 4314-4331 (2018). (23 citations) DOI: 10.1039/c7cs00650k.

P17. Impact of pH on Aqueous-Phase Phenol Hydrogenation Catalyzed by Carbon-Supported Pt and Rh, Nirala Singh, Mal-Soon Lee, Sneha A. Akhade, Guanhua Cheng, Donald M. Camaioni, Oliver Y. Gutiérrez, Vassiliki-Alexandra Glezakou, Roger Rousseau, Johannes A. Lercher and Charles T. Campbell, ***ACS Catalysis*** *9*, 1120-1128 (2019). DOI: 10.1021/acscatal.8b04039.

P18. Heats of Adsorption of N_2, CO, Ar and CH_4 versus Coverage on the Zr-Based MOF NU-

1000: Measurements and DFT Calculations, Graeme Vissers, Wei Zhang, Oscar E. Vilches, Wei-Guang Liu, Haoyu S. Yu, Donald G. Truhlar and Charles T. Campbell, ***Journal of Physical Chemistry C*** 123, 6586–6591 (2019). DOI: 10.1021/acs.jpcc.8b12263.

P19. Quantifying adsorption of organic molecules on platinum in aqueous phase by hydrogen site blocking and in situ X-ray absorption spectroscopy, Nirala Singh, Udishnu Sanyal, John L. Fulton, Oliver Y. Gutiérrez, Johannes A. Lercher and Charles T. Campbell, ***ACS Catalysis*** 9, 6869–6881 (2019). DOI: 10.1021/acscatal.9b01415.

P20. A Simple Bond-Additivity Model Explains Large Decreases in Heats of Adsorption in Solvents Versus Gas Phase: A Case Study with Phenol on Pt(111) in Water, Nirala Singh and Charles T. Campbell, ***ACS Catalysis*** 9, 8116–8127 (2019). DOI: 10.1021/acscatal.9b01870.

P21. Adhesion Energies of Solvent Films to Pt(111) and Ni(111) Surfaces by Adsorption Calorimetry, John R. Rumptz and Charles T. Campbell, ***ACS Catalysis*** 9, 11819−11825 (2019). DOI: 10.1021/acscatal.9b03591.

P22. Aqueous phase catalytic and electrocatalytic hydrogenation of phenol and benzaldehyde over platinum group metals, Nirala Singh; Udishnu Sanyal; Griffin Ruehl; Kelsey Stoerzinger; Oliver Y Gutiérrez; Donald M Camaioni; John L Fulton; Johannes A Lercher and Charles T Campbell, ***Journal of Catalysis*** 382, 372–384 (2020).

P23. Ni Nanoparticles on CeO_2(111): Energetics, Electron Transfer and Structure by Ni Adsorption Calorimetry, Spectroscopies and DFT, Zhongtian Mao, Pablo G. Lustemberg, John R. Rumptz, M. Verónica Ganduglia-Pirovano and Charles T. Campbell, *ACS Catalysis* **10**, 5101−5114 (2020).

P24. Catalytic Properties of Model Supported Nanoparticles, Charles T. Campbell, Nuria Lopez, and Stefan Vajda, *Journal of Chemical Physics* 152, 140401 (2020) (3 pages). https://doi.org/10.1063/5.0007579

P25. Silver Adsorption on Calcium Niobate(001) Nanosheets: Calorimetric Energies Explain Sinter-Resistant Support, Wei Zhang, Ritesh Uppuluri, Thomas E. Mallouk and Charles T. Campbell, *J. Am. Chem. Soc.* **142**, 15751−15763 (2020).

Other references cited:

1. Valden, M.; Lai, X.; Goodman, D. W., Onset of catalytic activity of gold clusters on titania with the appearance of nonmetallic properties. *Science* 1998**, 281**, 1647-1650.

2. Haruta, M., Size-and support-dependency in the catalysis of gold. *Catalysis Today* 1997**, 36**, 153.

3. Haruta, M., Catalysis of gold nanoparticles deposited on metal oxides. *Cattech* 2002**, 6**, 102-115.

4. Gunter, P. L. J.; Niemantsverdriet, J. W., Surface science approach to modeling supported catalysts. *Catal Rev-Sci Eng* 1997**, 39(1&2)**, 77.

5. Vaarkamp, M.; Miller, M. T.; Modica, F. S.; Koningsberger, D. C., On the relation between particle morphology, structure of the metal-support interface, and catalytic properties of Pt/gamma alumina. *J. Catal.* 1996**, 163**, 294.

6. Hayden, B. E.; Pletcher, D.; Suchsland, J. P.; Williams, L. J., The influence of support and particle size on the platinum catalysed oxygen reduction reaction. *Physical Chemistry Chemical Physics* 2009**, 11**, 9141-9148.

7. Judai, K.; Abbet, S.; Worz, A. S.; Heiz, U.; Henry, C. R., Low-temperature cluster catalysis. *Journal of the American Chemical Society* 2004**, 126**, 2732-2737.
8. Rodriguez, J. A.; Liu, P.; Hrbek, J.; Evans, J.; Perez, M., Water-Gas Shift Reaction on Cu and Au Nanoparticles Supported on CeO_2(111) and ZnO(000$^-$1): Intrinsic Reactivity and Importance of Support Interactions. *Angewante Chemie* 2007**, 46**, 1329-14.
9. Goodman, D. W., Model Studies in Catalysis Using Surface Science Probes. *Chemical Reviews* 1995**, 95**, 523-536.
10. Rodriguez, J. A.; Liu, P.; Wang, X.; Wen, W.; Hanson, J.; Hrbek, J.; Perez, M.; Evans, J., Water-gas shift activity of Cu surfaces and Cu nanoparticles supported on metal oxides. *Catalysis Today* 2009**, 143**, 45-50.
11. Deluga, G. A.; Salge, J. R.; Schmidt, L. D.; Verykios, X. E., Renewable hydrogen from ethanol by autothermal reforming. *Science* 2004**, 303**, 993-997.
12. Schubert, M. M. H., S.; VanVeen, A.C.; Muhler, M.; Plzak, V.; Behm, R.J., CO oxidation over supported gold catalysts-"inert" and "active" support materials and their role for oxygen supply during reaction. *J. Catal.* 2001**, 197**, 113-22.
13. Chen, M. S.; Goodman, D. W., Catalytically active gold: From nanoparticles to ultrathin films. *Accounts of Chemical Research* 2006**, 39**, 739-746.
14. Lei, Y.; Mehmood, F.; Lee, S.; Greeley, J.; Lee, B.; Seifert, S.; Winans, R. E.; Elam, J. W.; Meyer, R. J.; Redfern, P. C.; Teschner, D.; Schlogl, R.; Pellin, M. J.; Curtiss, L. A.; Vajda, S., Increased Silver Activity for Direct Propylene Epoxidation via Subnanometer Size Effects. *Science* 2010**, 328**, 224-228.
15. Min, M. K.; Cho, J. H.; Cho, K. W.; Kim, H., Particle size and alloying effects of Pt-based alloy catalysts for fuel cell applications. *Electrochimica Acta* 2000**, 45**, 4211-4217.
16. Silva, C. G.; Juarez, R.; Marino, T.; Molinari, R.; Garcia, H., Influence of Excitation Wavelength (UV or Visible Light) on the Photocatalytic Activity of Titania Containing Gold Nanoparticles for the Generation of Hydrogen or Oxygen from Water. *Journal of the American Chemical Society* 2011**, 133**, 595-602.
17. Bezemer, G. L.; Bitter, J. H.; Kuipers, H.; Oosterbeek, H.; Holewijn, J. E.; Xu, X. D.; Kapteijn, F.; van Dillen, A. J.; de Jong, K. P., Cobalt particle size effects in the Fischer-Tropsch reaction studied with carbon nanofiber supported catalysts. *Journal of the American Chemical Society* 2006**, 128**, 3956-3964.
18. Campbell, C. T.; Sellers, J. R. V., Anchored metal nanoparticles: Effects of support and size on their energy, sintering resistance and reactivity. *Faraday Discussions* 2013**, 162**, 9-30.
19. Campbell, C. T., The Energetics of Supported Metal Nanoparticles: Relationships to Sintering Rates and Catalytic Activity. *Accounts of Chemical Research* 2013**, 46**, 1712-1719.
20. Campbell, C. T.; Sharp, J. C.; Yao, Y. X.; Karp, E. M.; Silbaugh, T. L., Insights into catalysis by gold nanoparticles and their support effects through surface science studies of model catalysts. *Faraday Discussions* 2011**, 152**, 227-239.
21. Parker, S. C.; Campbell, C. T., Kinetic model for sintering of supported metal particles with improved size-dependent energetics and applications to Au on TiO2(110). *Physical Review B* 2007**, 75**, 035430.
22. Campbell, C. T.; Parker, S. C.; Starr, D. E., The effect of size-dependent nanoparticle energetics on catalyst sintering. *Science* 2002**, 298**, 811-814.
23. Hansen, T. W.; Delariva, A. T.; Challa, S. R.; Datye, A. K., Sintering of Catalytic Nanoparticles: Particle Migration or Ostwald Ripening? *Accounts of Chemical Research* 2013**, 46**, 1720-1730.

24. Jones, J.; Xiong, H. F.; Delariva, A. T.; Peterson, E. J.; Pham, H.; Challa, S. R.; Qi, G. S.; Oh, S.; Wiebenga, M. H.; Hernandez, X. I. P.; Wang, Y.; Datye, A. K., Thermally stable single-atom platinum-on-ceria catalysts via atom trapping. *Science* 2016**, 353**, 150-154.
25. Borup, R. L.; Davey, J. R.; Garzon, F. H.; Wood, D. L.; Inbody, M. A., PEM fuel cell electrocatalyst durability measurements. *Journal of Power Sources* 2006**, 163**, 76-81.
26. Addou, R.; Senftle, T. P.; O'Connor, N.; Janik, M. J.; van Duin, A. C. T.; Batzill, M., Influence of Hydroxyls on Pd Atom Mobility and Clustering on Rutile TiO2(011)-2 x 1. *ACS Nano* 2014**, 8**, 6321-6333.
27. Hejral, U.; Muller, P.; Balmes, O.; Pontoni, D.; Stierle, A., Tracking the shape-dependent sintering of platinum-rhodium model catalysts under operando conditions. *Nature Communications* 2016**, 7**, 10964.
28. Lee, S.; Seo, J.; Jung, W., Sintering-resistant Pt@CeO2 nanoparticles for high-temperature oxidation catalysis. *Nanoscale* 2016**, 8**, 10219-10228.
29. Zhang, J.; Wang, L.; Zhang, B. S.; Zhao, H. S.; Kolb, U.; Zhu, Y. H.; Liu, L. M.; Han, Y.; Wang, G. X.; Wang, C. T.; Su, D. S.; Gates, B. C.; Xiao, F. S., Sinter-resistant metal nanoparticle catalysts achieved by immobilization within zeolite crystals via seed-directed growth. *Nature Catalysis* 2018**, 1**, 540-546.
30. Parker, S. C.; Campbell, C. T., Reactivity and sintering kinetics of Au/TiO2(110) model catalysts: particle size effects. *Topics in Catalysis* 2007**, 44**, 3-13.
31. Wynblatt, P.; Gjostein, N. A., Supported metal crystallites. In *Progess in Solid State Chemistry*, McCaldin, J. O.; Somorjai, G. A., Eds. Pergamon: Oxford, 1975; Vol. 9, p 21.
32. Farmer, J. A.; Campbell, C. T., Ceria Maintains Smaller Metal Catalyst Particles by Strong Metal-Support Bonding. *Science* 2010**, 329**, 933-936.
33. Houk, L. R.; Challa, S. R.; Grayson, B.; Fanson, P.; Datye, A. K., The Definition of "Critical Radius" for a Collection of Nanoparticles Undergoing Ostwald Ripening. *Langmuir* 2009**, 25**, 11225-11227.
34. Hemmingson, S. L.; Campbell, C. T., Trends in Adhesion Energies of Metal Nanoparticles on Oxide Surfaces: Understanding Support Effects in Catalysis and Nanotechnology. *ACS Nano* 2017**, 11**, 1196-1203.
35. den Breejen, J. P.; Radstake, P. B.; Bezemer, G. L.; Bitter, J. H.; Froseth, V.; Holmen, A.; de Jong, K. P., On the Origin of the Cobalt Particle Size Effects in Fischer-Tropsch Catalysis. *Journal of the American Chemical Society* 2009**, 131**, 7197-7203.
36. Li, L.; Larsen, A. H.; Romero, N. A.; Morozov, V. A.; Glinsvad, C.; Abild-Pedersen, F.; Greeley, J.; Jacobsen, K. W.; Norskov, J. K., Investigation of Catalytic Finite-Size-Effects of Platinum Metal Clusters. *Journal of Physical Chemistry Letters* 2013**, 4**, 222-226.
37. Kleis, J.; Greeley, J.; Romero, N. A.; Morozov, V. A.; Falsig, H.; Larsen, A. H.; Lu, J.; Mortensen, J. J.; Dulak, M.; Thygesen, K. S.; Norskov, J. K.; Jacobsen, K. W., Finite Size Effects in Chemical Bonding: From Small Clusters to Solids. *Catalysis Letters* 2011**, 141**, 1067-1071.
38. Campbell, C. T., Bimetallic Model Catalysts. In *The Handbook of Heterogeneous Catalysis,*, Ertl, G., Knözinger, H. and Weitkamp, J., Ed. VCH: Weinhein, Germany, 1997; pp 814-826.
39. Campbell, C. T.; Mao, Z. T., Chemical Potential of Metal Atoms in Supported Nanoparticles: Dependence upon Particle Size and Support. *ACS Catalysis* 2017**, 7**, 8460-8466.
40. Rodriguez, J. A.; Goodman, D. W., THE NATURE OF THE METAL METAL BOND IN BIMETALLIC SURFACES. *Science* 1992**, 257**, 897-903.

41. Roling, L. T.; Abild-Pedersen, F., Structure-Sensitive Scaling Relations: Adsorption Energies from Surface Site Stability. *Chemcatchem* 2018**, 10**, 1643-1650.
42. Mostafa, S.; Behafarid, F.; Croy, J. R.; Ono, L. K.; Li, L.; Yang, J. C.; Frenkel, A. I.; Roldan Cuenya, B., Shape-Dependent Catalytic Properties of Pt Nanoparticles. *Journal of the American Chemical Society* 2010**, 132**, 15714-15719.
43. Roldan Cuenya, B., Metal Nanoparticle Catalysts Beginning to Shape-up. *Accounts of Chemical Research* 2013**, 46**, 1682-1691.
44. Roldan Cuenya, B.; Behafarid, F., Nanocatalysis: size- and shape-dependent chemisorption and catalytic reactivity. *Surface Science Reports* 2015**, 70**, 135-187.
45. Xu, L. J.; Henkelman, G.; Campbell, C. T.; Jonsson, H., Small Pd clusters, up to the tetramer at least, are highly mobile on the MgO(100) surface. *Physical Review Letters* 2005**, 95**, Art. No. 146103.
46. Branda, M. M.; Hernandez, N. C.; Sanz, J. F.; Illas, F., Density Functional Theory Study of the Interaction of Cu, Ag, and Au Atoms with the Regular CeO2 (111) Surface. *Journal of Physical Chemistry C* 2010**, 114**, 1934-1941.
47. O'Connor, N. J.; Jonayat, A. S. M.; Janik, M. J.; Senftle, T. P., Interaction trends between single metal atoms and oxide supports identified with density functional theory and statistical learning. *Nature Catalysis* 2018**, 1**, 531-539.